Focus Article

Tensor decompositions and data fusion in epileptic electroencephalography and functional magnetic resonance imaging data

Borbála Hunyadi,[1,2] Patrick Dupont,[3] Wim Van Paesschen[4] and Sabine Van Huffel[1,2]*

Electroencephalography (EEG) and functional magnetic resonance imaging (fMRI) record a mixture of ongoing neural processes, physiological and nonphysiological noise. The pattern of interest, such as epileptic activity, is often hidden within this noisy mixture. Therefore, blind source separation (BSS) techniques, which can retrieve the activity pattern of each underlying source, are very useful. Tensor decomposition techniques are very well suited to solve the BSS problem, as they provide a unique solution under mild constraints. Uniqueness is crucial for an unambiguous interpretation of the components, matching them to true neural processes and characterizing them using the component signatures. Moreover, tensors provide a natural representation of the inherently multidimensional EEG and fMRI, and preserve the structural information defined by the interdependencies among the various modes such as channels, time, patients, etc. Despite the well-developed theoretical framework, tensor-based analysis of real, large-scale clinical datasets is still scarce. Indeed, the application of tensor methods is not straightforward. Finding an appropriate tensor representation, suitable tensor model, and interpretation are application dependent choices, which require expertise both in neuroscience and in multilinear algebra. The aim of this paper is to provide a general guideline for these choices and illustrate them through successful applications in epilepsy.

How to cite this article:
WIREs Data Mining Knowl Discov 2017, 7:e1197. doi: 10.1002/widm.1197

INTRODUCTION

Epilepsy, affecting 0.5–1% of the world population, is a wide spectrum of neurological disorders, characterized by recurrent epileptic seizures, which arise due to abnormal electrical activity in the brain. The causes, symptoms, and severity of the disease vary drastically among individual patients. Therefore, precise diagnosis, i.e., establishing the exact type of epilepsy, is a crucial factor in choosing proper treatment. The gold standard for diagnosing epilepsy is electroencephalogram (EEG) monitoring. The absence or presence of certain characteristic

*Correspondence to: sabine.vanhuffel@esat.kuleuven.be

[1]Stadius Center for Dynamical Systems, Signal Processing and Data Analytics, Department of Electrical Engineering, KU Leuven, Leuven, Belgium

[2]iMinds Medical IT, Leuven, Belgium

[3]Laboratory of Cognitive Neurology, KU Leuven and UZ Leuven, Leuven, Belgium

[4]Laboratory for Epilepsy Research, KU Leuven and UZ Leuven, Leuven, Belgium

Conflict of interest: The authors have declared no conflicts of interest for this article.

patterns in the EEG can differentiate epileptic seizures from seizure-like symptoms of different origin. After establishing the diagnosis, antiepileptic drug treatment can be initiated. Unfortunately, in approximately 30% of all epilepsy patients, the seizure cannot be controlled by medication. In such cases, epilepsy surgery may be considered in order to resect or disconnect the region responsible for generating the seizures, i.e., the epileptogenic zone (EZ). To localize the EZ, different imaging modalities can be used besides EEG monitoring such as magnetic resonance imaging (MRI), functional MRI (fMRI), positron emission tomography (PET), or single-photon emission computed tomography (SPECT). In this paper, we will focus on EEG and fMRI analysis methods to support the diagnostic procedure of epilepsy.

Technically speaking, several preliminary considerations can be made regarding the choice of the analysis techniques. First of all, given the fact that each and every epilepsy case is unique, data-driven approaches should be implemented. Furthermore, the chosen technique has to efficiently handle large multivariate datasets, i.e., EEG and fMRI signals sampled during a long period at different spatial locations. Robustness against noise is another crucial aspect. Indeed, EEG and fMRI measure a mixture of signals originating from different physiological and nonphysiological processes, which are all superimposed on the epileptic signal pattern.

With this in mind, different blind source separation (BSS) techniques have been extensively and successfully used to mine epileptic EEG and fMRI data. BSS techniques consider a set of observations, which arise from a mixture of underlying source signals and aim to recover the sources and the mixing system blindly, i.e., only based on the available observations. The majority of BSS techniques achieves this goal and ensures a unique solution by imposing certain constraints on the sources or the mixing system. In order to interpret the results and take them into account in the medical diagnostic procedure, it is crucial that the solution is unique and the constraints are biologically plausible.

Multichannel signals are naturally represented in a matrix, where each row of the matrix contains the signal measured by each sensor. Matrices are also called two-way arrays, expressing variability in time and space (sensors) along the two dimensions. Tensors are higher-order generalizations of matrices, i.e., multiway arrays, which can represent additional types of variability in their higher dimensions. For example, data recorded from different patients can be organized along the third dimension. A fourth dimension may arise from the mathematical manipulation of the signal, with the intention of conveying relevant information about the signals, such as spectral information through frequency transformation. In case of multiway data, BSS can be formulated as a tensor decomposition problem. Remarkably, tensor decomposition techniques offer a unique solution under mild conditions, making them a very desirable method to solve the BSS problem.

The goal of this paper is to highlight the strengths of tensor-based BSS techniques through successful examples, propose new directions, and encourage continued efforts within the field of epilepsy research, neuroimaging, and beyond.

The paper is organized as follows. In section *Mining EEG and fMRI in Epilepsy*, we discuss some challenging tasks where knowledge discovery through BSS can help answer clinical questions related to epilepsy. In section *BSS Multiway Data*, we give a formal definition to BSS, introduce the most important tensor decomposition techniques and discuss their uniqueness properties. In section *Tensor Analysis of Functional Brain Data: A General Framework*, we give a general framework for tensor-based analysis of EEG and fMRI. Finally, in section *Tensor Analysis of Epileptic EEG and fMRI: Successful Applications*, we review the existing tensor-based solutions, which have successfully tackled clinical or research questions in the field of epilepsy.

MINING EEG AND fMRI IN EPILEPSY

Epilepsy affects brain function, causing pathological changes in brain activity. EEG and fMRI record continuous data from the functioning brain over a certain period, therefore, can capture epileptic activity as well. Besides epileptic activity, normal neural activity, other physiological signals, and nonphysiological noise are also recorded. Therefore, it is not trivial to answer the crucial questions: when and where does epileptic activity take place.

The EEG recordings may last up to 1 week, when the patients are hospitalized for presurgical evaluation. Although trained experts can recognize epileptic EEG patterns visually, reviewing such large amounts of data is very time consuming. Therefore, *automated seizure detection* techniques are very beneficial in long-term monitoring. Once the seizure occurrences have been identified, the EEG data are further analyzed in order to determine the seizure onset zone (SOZ). Practically, this means finding the electrode on which the first signs of ictal pattern are seen. As seizures are often accompanied by involuntary muscle contractions, severe artifacts often contaminate the ictal pattern hindering visual interpretation. Therefore,

BSS techniques for *artifact removal* or for modeling the source of interest are crucial. Note, however, that the spatial resolution of scalp EEG is relatively low. For precise delineation of the SOZ, we need *source imaging techniques*[1] to map the data from the channel space to the source space, i.e., obtain three dimensional (3D) localization information.

Alternatively, fMRI offers high spatial resolution by measuring blood-oxygen-level dependent (BOLD) signals at typically $3 \times 3 \times 3$ mm^3 voxels within the whole volume of the brain. To determine the brain regions that are involved in generating epileptic activity, fMRI signals are usually analyzed in conjunction with temporal information from simultaneously recorded EEG. *EEG–fMRI integration* poses various signal processing challenges, such as removing severe scanner artifacts from the EEG,[2] reliably identifying interictal epileptic discharges[3,4] and accounting for the mismatch in terms of the temporal dynamics and the spatiotemporal resolution between the EEG and fMRI signals.[5,6]

More recent approaches to unravel epilepsy-related neural phenomena are based on studying the interactions among the brain signals recorded at different spatial locations. *Functional connectivity analysis* studies the statistical interdependency between the multivariate brain signals. It can reveal the origin and the spreading pattern on epileptic activity in EEG[7] or study large-scale network behavior and disruption in fMRI, which can lead to a better understanding of the disease mechanisms.[8]

Besides studying pathological phenomena, fMRI also plays an important role in mapping healthy brain function to determining the eloquent cortex, i.e., regions that are responsible for memory, sensory, motor, and language function.[9]

BSS OF MULTIWAY DATA

Blind Source Separation

There are a few common elements among the above-discussed signal processing challenges. They all tackle large multichannel time series of low signal to noise ratio, where the pattern of interest is embedded in a mixture of irrelevant information. Formally, let $s_{r^*} \in \mathbb{R}^I$, a real vector of length I, denote the source of interest, and $s_1, \ldots s_{r-1}, s_{r+1}, \ldots s_R \in \mathbb{R}^I$ are other physiological and nonphysiological sources. Depending on the location of the sources with respect to the spatial sampling points (EEG channels or fMRI voxels), they contribute to the measured signals with different weights $a_1, \ldots a_R \in \mathbb{R}^J$ Then, the observed multichannel signal $X \in \mathbb{R}^{I \times J}$ can be written as a linear instantaneous mixture of the sources, where the mixing system is defined by the weights:

$$X = \sum_{r=1}^{R} a_r s_r^T + E = \sum_{r=1}^{R} a_r \circ s_r + E = AS + E. \quad (1)$$

The goal of BSS is to recover the sources and the mixing system purely based on the observations and characterize the source of interest based on the temporal and spatial signatures s_{r^*} and a_{r^*}. In other words, the aim is to factorize the matrix X in interpretable rank-1 components. Different terminology calls the mixing matrix A and source matrix S factor matrices. Furthermore, we will call their respective columns and rows signatures. The outer product (denoted by $\circ$) of the signatures defines the components. Some BSS models are exact and will model noise as an additional source variable, while others allow a residual error term E.

Interpretability implies that the factorization problem is unique. This guarantees the extraction of a unique set of sources, the signatures of which need to match as closely as possible to those of the true sources. However, the matrix factorization problem, in general, does not produce a unique solution.[10] Additional constraints, such as orthogonality or statistical independence of the sources are imposed in order to ensure uniqueness. However, in general, there is no reason to assume that true physiological processes behave independently in the brain. Instead, they behave as a highly complex system of interconnected regions, which dynamically interact and modulate each others' activity.

Tensor Factorization

Let us generalize the matrix factorization problem to the case of a Nth order tensor $\mathcal{X} \in \mathbb{R}^{I_1 \times I_2 \times \cdots \times I_N}$:

$$\mathcal{X} = \sum_{r=1}^{R} a_r^{(1)} \circ a_r^{(2)} \circ \cdots \circ a_r^{(N)} + E. \quad (2)$$

This model is called the polyadic decomposition (PD). The smallest R for which $E = 0$ is called the rank of the tensor, and the model is the *canonical polyadic decomposition* (CPD). CPD is a very powerful tool for BSS, as the conditions under which it is unique, are easily met. Later we discuss two sufficient conditions for uniqueness.

A very simple and easy to check condition, which often applies in BSS problems, states that the CPD of a third-order tensor is unique if two factor

matrices have linearly independent columns and the third factor matrix has no collinear columns.

The most well-known and more relaxed uniqueness condition, first derived by Kruskal[11] for third-order tensors and later generalized to higher order tensors by Sidiropoulos and Bro[12] relates the number of components to the number of collinear columns in the factor matrices:

$$k_{A^{(1)}} + k_{A^{(2)}} + k_{A^{(3)}} \geq 2R + 2, \tag{3}$$

where k_A denotes the k-rank of the matrix, defined as the largest number of k such that any k columns of A are linearly independent, and $A^{(i)}$ denotes the factor matrix comprising the signatures in mode i. Some of the most relaxed general conditions for uniqueness were introduced recently in a comprehensive study by Refs 13,14. Note that the unique decomposition is subject to trivial indeterminacies, therefore, the ordering or the magnitude of the extracted signatures cannot be interpreted.

Note that rank-1 CPD terms imply trilinear components, i.e., in each source, the same signature pattern is scaled along the other two modes. In certain cases, this model might be too restrictive and does not match the true physical properties of the underlying sources. *Block term decompositions* (BTDs) offer more flexible models through extracting low-rank components, rather than rank-1 components.[15] In this review, we will discuss one particular case, block term decomposition of a third-order tensor $\mathcal{X} \in \mathbb{R}^{I_1 \times I_2 \times I_3}$ in rank-$(L_r,L_r,1)$ components:

$$\mathcal{X} = \sum_{r=1}^{R} \left(A_r^{(1)} \cdot \left(A_r^{(2)} \right)^T \right) \circ a_r^{(3)}. \tag{4}$$

The matrix $D_r = A_r^{(1)} \cdot \left(A_r^{(2)} \right)^T \in \mathbb{R}^{I_1 \times I_2}$ has rank L_r, and the vector $a_r^{(3)}$ is nonzero. Similarly to CPD, this decomposition has mild uniqueness conditions up to trivial indeterminacies. In case the matrices $\left[A_1^{(1)} \ldots A_R^{(1)} \right]$ and $\left[A_1^{(2)} \ldots A_R^{(2)} \right]$ have linearly independent columns, and the matrix $\left[a_1^{(3)} \ldots a_R^{(3)} \right]$ has no collinear columns, the decomposition is guaranteed to be unique. For more relaxed uniqueness conditions, we refer the reader to [16,17]

Both CPD and BTD can be viewed as a constrained *Tucker decomposition*. In the Tucker model, the tensor is written as the product of a core tensor and the factor matrices:

$$\mathcal{X} = \mathcal{G} \times_1 A^{(1)} \times_1 A^{(2)} \cdots \times_1 A^{(N)}. \tag{5}$$

The values in the core tensor control the interactions between the factor signatures: in case of the trilinear CPD, only the values on the superdiagonal are nonzero, while BTD allows some off-diagonal nonzeros depending on the multilinear rank of the components. While Tucker decompositions offer very good model fit, they have many degrees of freedom, therefore, the nonunique factors usually have no physical meaning.

An illustration of the various tensor decompositions is shown in Figure 1.

Coupled Tensor Factorization

Often more than one sort of measurements is performed to study different aspects of the same phenomenon. For example, the electromagnetic waves generated in the brain can be measured with EEG or MEG. BOLD signal changes in active tissue are captured by fMRI. Metabolic changes, perfusion,

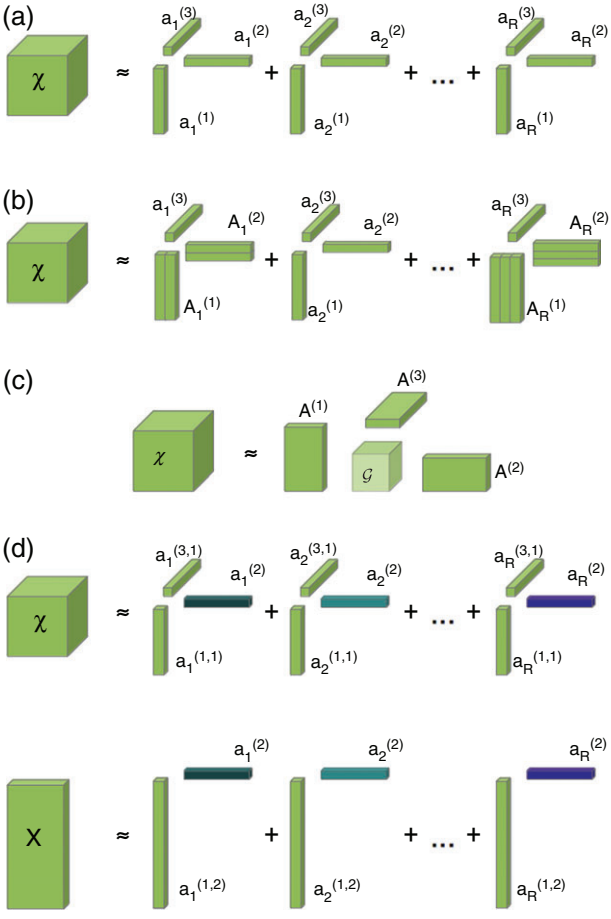

FIGURE 1 | Illustration of the most important tensor decompositions: (a) CPD, (b) BTD-(L_r,L_r,1), (c) Tucker, (d) CMTF. CPD, canonical polyadic decomposition; BTD, block term decomposition; CMTF, coupled matrix-tensor factorization.

structural connections, or anatomy can be acquired using PET, SPECT, diffusion imaging, or structural MR, respectively. The integration of the information coming from these complementary modalities is highly beneficial to obtain a more detailed characterization of the underlying processes. Often these measurements share one or more common source of variability. For example, the same underlying neural source will generate a similar temporal pattern in EEG and MEG. Owing to some pathology, changes occurring in similar brain regions will be captured using the different modalities, hence, the images will share similar spatial signature. Or, in case of a multisubject dataset, the subject-by-subject variability will be related in all modalities. One can exploit this common variability using joint BSS. Joint independent component analysis (jointICA) is a matrix-based technique, which concatenates the data from each modality into a large matrix. Then, assuming that the underlying sources are mutually statistically independent, and that the exact same mixing system A generates the observations, it concatenates the data from all modalities into a large source matrix $\left[X^{[mod_1]}\ X^{[mod_2]}\ldots X^{[mod_K]}\right]$, and retrieves the joint sources $\left[S^{[mod_1]}\,S^{[mod_2]}\ldots S^{[mod_K]}\right]$ using ICA [18,19]:

$$\left[X^{[mod_1]}\ X^{[mod_2]}\ldots X^{[mod_K]}\right] = A\left[S^{[mod_1]}\,S^{[mod_2]}\ldots S^{[mod_K]}\right]. \tag{6}$$

The strong assumption of the same underlying mixing system for all modalities can be relaxed by preprocessing the dataset using multimodal CCA.[20]

Similarly to the unimodal case discussed previously, tensor-based techniques, which jointly factorize two or more tensors, can circumvent the independence constraint in joint BSS. Let us consider a set of m tensors $\mathcal{X}^m \in \mathbb{R}^{I_1 \times I_{2,m} \times \cdots \times I_{K_m,m}}$, $m \in \{1,\ldots,M\}$, where each tensor may have different order K_m and different sizes $I_{K_m,m}$, except for the first dimension, which is of size I_1 and is shared among all tensors. The coupled PD of this set of tensors is formulated as follows:

$$\mathcal{X}^m = \sum_{r=1}^{R} a_r^{(1)} \circ a_r^{(2,m)} \circ \cdots \circ a_r^{(K_m,m)}. \tag{7}$$

Interestingly, the uniqueness conditions for a coupled decomposition are even more relaxed than the conditions for the decomposition of the single tensors.[21] One special case, namely coupled matrix-tensor factorization (CMTF) has been studied extensively in the literature and has found different applications in EEG–fMRI analysis and beyond.[22] Let us consider a matrix $X \in \mathbb{R}^{I_1 \times I_2}$ and a third-order tensor $\mathcal{X} \in \mathbb{R}^{I_1 \times I_2 \times I_3}$. Their coupled decomposition is written as:

$$\begin{aligned} X &= \sum_{r=1}^{R} a_r^{(1)} \circ a_r^{(2,1)} \\ \mathcal{X} &= \sum_{r=1}^{R} a_r^{(1)} \circ a_r^{(2,2)} \circ a_r^{(3,2)} \end{aligned} \tag{8}$$

Regarding the uniqueness of the factors A^1, $A^{2,2}$, and $A^{3,2}$, the same mild conditions hold as in CPD. In order to ensure the uniqueness of $A^{2,1}$, the common factor matrix A^1 needs to have full column rank.[21]

Similarly to jointICA, this model assumes that the factors in the shared dimension are equal. Several relaxations of this condition have been proposed, such as advanced CMTF (ACMTF), which allow the existence of both shared and nonshared factors,[5,22] or relaxed ACMTF, which allows similarity rather than equivalence of the shared factors.[23] Alternatively, multiway partial least squares (N-PLS) can be applied, which generalizes the concept of PLS regression. In a resting state EEG–fMRI experiment, the electrical and BOLD signal sources were estimated such that the shared temporal signatures in both modalities have maximal covariance.[24]

TENSOR ANALYSIS OF FUNCTIONAL BRAIN DATA: A GENERAL FRAMEWORK

In this section, we provide a comprehensive guide on performing tensor-based analysis of EEG and fMRI data. Each step of the processing pipeline is discussed in detail in order to highlight the necessary considerations and identify possible decisions. We will illustrate each step using an example EEG segment recorded during an epileptic seizure. Data were analyzed in Matlab R2014a with built-in routines, Tensorlab[25] and the N-way toolbox,[26] two Matlab toolboxes for tensor manipulations and decompositions.

Figure 2 summarizes the consecutive steps of the processing pipeline.

In the first *tensorization* step, the data are preprocessed and organized in the form of a higher order array. Such a representation may come naturally, for instance when multichannel measurements are performed repeatedly or in different patients. The multichannel signal forms a matrix; repeated measurements organized along the third dimension form a third-order tensor; finally, such repeated

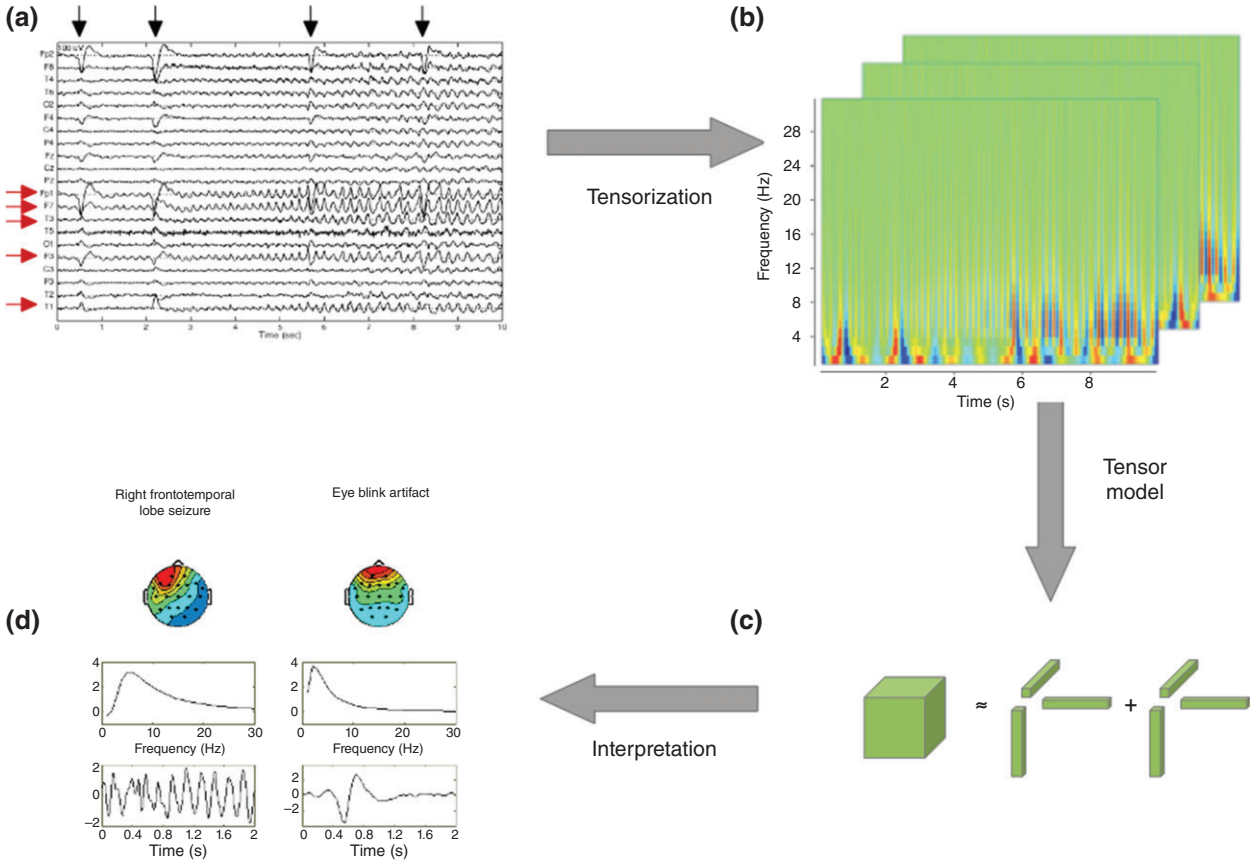

FIGURE 2 | Tensor-based EEG and fMRI data analysis include the following steps: data tensorization, tensor model selection and computation, and interpretation. (a) A 10-second long EEG segment with clear oscillatory ictal pattern. (b) Third-order EEG tensor with dimensions channels × time × frequency, obtained by wavelet transform. (c) Schematic of a CPD model with R = 2. (d) Signatures of the components extracted from the first 2 second of the ictal pattern. The channel signatures are conveniently visualized as topographical images interpolated over a two dimensional (2D) image of the head from a top viewpoint in radiological convention, i.e., the left of the patient is in the right of the image. Red, green, and blue colors indicate positive, zero, and negative values, respectively. EEG, electroencephalography; fMRI, functional magnetic resonance imaging; CPD, canonical polyadic decomposition.

measurements performed on multiple patients will give rise to a fourth-order tensor with dimensions *channels* × *time samples* × *measurements* × *patients*.

Alternatively, an additional dimension may arise from the mathematical manipulation of the signal. The motivation for this is twofold. First, in case there is prior knowledge or a reasonable assumption about the properties of the underlying sources, such mathematical manipulation can convey this knowledge about the signals. Second, a well-chosen transformation will result in a low-rank data structure, which will make the data suitable for tensor decomposition. Therefore, tensorization is a crucial and application dependent step, which requires both biomedical and mathematical expertise.

Wavelet transformation and other time–frequency transformations are very popular in EEG signal processing. Many different types of neural phenomena appear as an oscillatory signal in a certain frequency band, such as $\propto$ activity,[24] epileptic seizures,[27,28] or event-related synchronization and desynchronization. The time–frequency representation of a neural oscillation will result in a rank-1 tensor in case the oscillatory source remains at the same location and maintains the same frequency; while changes in either of these properties will give rise to a low-rank tensor. On the contrary, muscle artifacts have a very broad frequency spectrum and a high multilinear rank. As such, they cannot be modeled using a tensor decomposition in low-rank terms. As an example, a 10-second long segment of an epileptic seizure recorded by EEG is visualized in Figure 2(a). Red arrows indicate the channels on which the ictal (seizure) pattern is most pronounced. Black arrows indicate eye blink artifacts. In Figure 2(b), we show the corresponding tensor representation obtained by

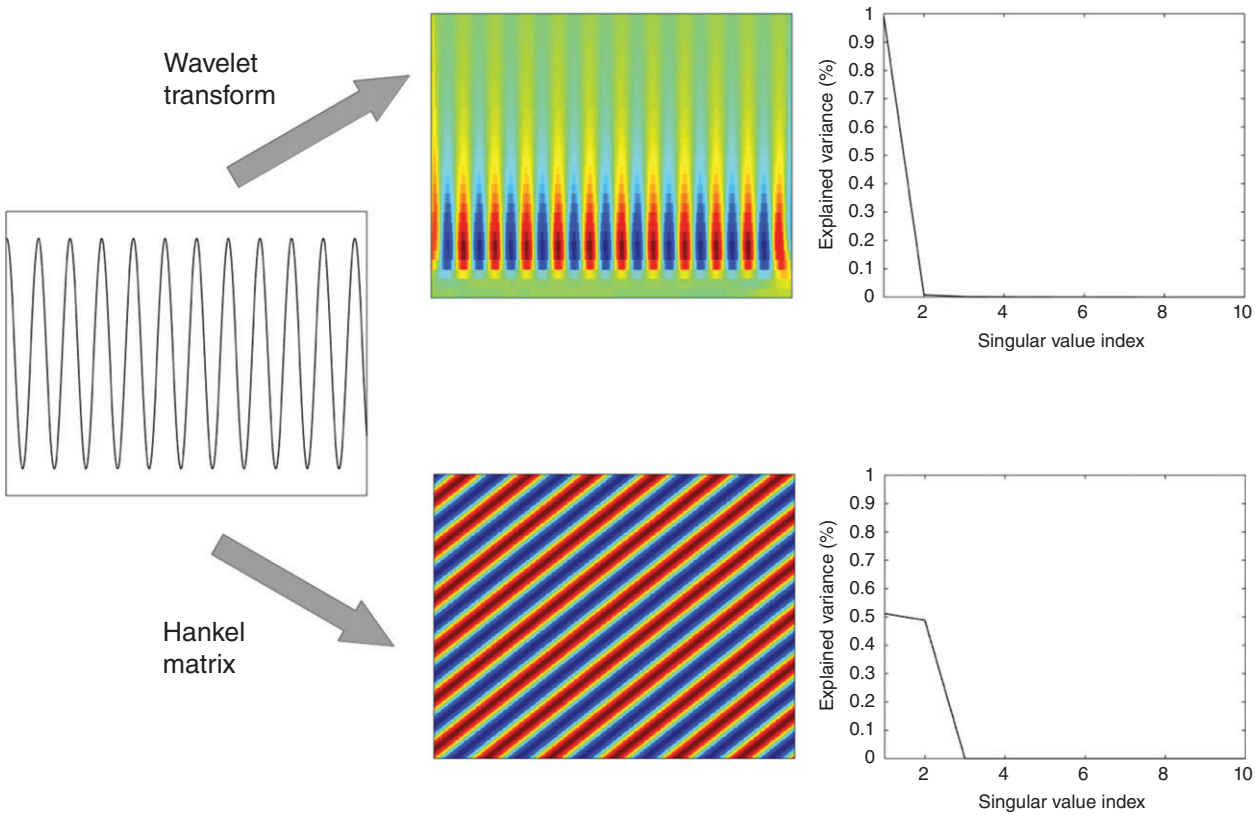

FIGURE 3 | The appropriate tensor model depends on the chosen tensor representation, as the exact same source pattern can have different rank using different representations. For example, a sinusoidal source pattern (left panel) is approximately rank-1 using wavelet transformation (top middle), while its corresponding Hankel matrix (bottom middle) is rank-2, as shown by the singular value spectrum of the matrices (right top and bottom, respectively).

wavelet transformation. The oscillatory pattern, which increases in amplitude toward the end of the EEG segment, is the epileptic seizure activity. In the wavelet tensor, this pattern is reflected as large coefficients between 4 and 8 Hz after 5 second. Large coefficients at lower frequencies reflect eye blink artifact, observed at 0.5, 2, 6, and 8 second.

Brain oscillations and rhythms are well approximates as the sum of sinusoids, i.e., a sum of exponentials. Let us consider the representation of the signal in a Hankel matrix, where the entries along the skew-diagonal are constant and correspond to the consecutive time samples of the signal. It is well-known in system identification, that the Hankel matrix of a pure exponential is rank-1, that of a sinusoid (sum of two exponentials) is rank-2. In general, an exponential polynomial of degree L yields a Hankel matrix of rank L. Therefore, neural sources represented in Hankel matrices will admit a low-rank tensor decomposition.[15]

Many further tensorization schemes exist, which have not yet found an application in biomedical signal processing, which, however, may be of interest. For example, sources, which can be approximated as rational functions, yield low-rank Löwner matrices. For additional examples and detailed theoretical explanation, we refer the reader to Ref 29.

The second step of the processing pipeline is the *selection and computation of the appropriate tensor model* for decomposition. The suitable tensor model strongly depends on the chosen tensor representation. As illustrated in Figure 3, the exact same source will have different rank using different representations; therefore, it requires a different tensor model.

Several techniques exist to assist model selection. The first group of techniques aims to find a trade-off between model complexity and fit, e.g., DIFFIT.[30] Naturally, the more complex the model (higher number and higher multilinear rank components), the better the model fit. Automated methods study the changes of the model fit in function of the parameters and then choose the corner or the saturation point of the curve, where increasing

model complexity does not improve the fit considerably. Such techniques tend to overestimate the model complexity of EEG and fMRI data. At reasonable signal-to-noise ratio, if an appropriate low-rank representation is chosen taking into account the properties of the source of interest, this source will be represented using a relatively few number of components. Adding more components to the model will usually not improve the reconstruction of the source of interest, but will only model noise and sources of no interest.

Another widely used technique, called core consistency diagnostic [31] tests the validity of the hypothesized CPD or other restricted Tucker models *post hoc*. More specifically, it fits the data onto the computed factors in the least squares sense, and then compares the resulting core tensor to the hypothesized core tensor. In case of CPD, the core consistency of the fitted model is computed for increasing number of models. Then, the suggested number of components is the last in the row, which still yields a core consistency close to 100%. This approach has successfully been used in several EEG applications, e.g., see Refs 32,33.

We encourage the reader to use a combination of different techniques and consider background knowledge from the application field to make an informed decision.

We illustrate the model selection procedure on the initial 2-second long segment of the EEG visualized in Figure 2, i.e., at the onset of the seizure. A tensor was obtained using a wavelet transformation.

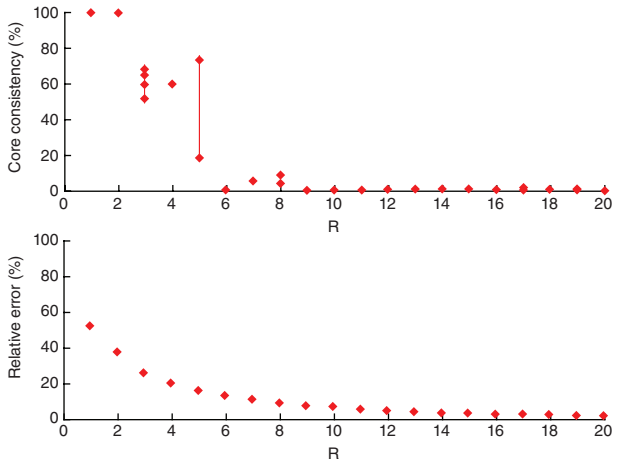

FIGURE 4 | CPD model selection for the first 2-second long segment of EEG data visualized in Figure 2, tensorized using wavelet transformation. The core consistency (top) and explained variance (bottom) are shown for five randomly initialized CPD models with different ranks ranging from 1 to 20. CPD, canonical polyadic decomposition; EEG, electroencephalography.

A CPD model with different ranks ranging from 1 to 20 was run five times with random initializations. The core consistency and the relative error of each CPD is shown in Figure 4. A rank-1 CPD model explains around half of the total variance of the signal. The relative error drops sharply by increasing the rank until 3 or 4, then it keeps decreasing moderately. At the same time, the core consistency shows a perfect trilinear structure up to rank-2, while the lower values for rank-3, rank-4, and rank-5 indicate that there is a considerable amount of variance in the data which is not trilinear. Models with a rank higher than 6 are invalid. Therefore, a rank-2 CPD model seems to be a good choice for this data. Visual inspection of the original segment reinforces this decision, as two different physiological patterns were observed in the EEG, namely seizure activity and eye blinks.

Different computational schemes have been developed for performing tensor decomposition. For an overview, we refer the reader to Ref 34.

The final step involves the *interpretation* of the resulting components. As we have explained earlier, the uniqueness of the decomposition is essential for unambiguous interpretation. In case the factors are not unique, the interpretation of an arbitrarily chosen solution may lead to false conclusions. As explained above, they are easily checked and met conditions, under which a tensor decomposition in unique. In the noiseless case, the unique solution can be explicitly computed using linear algebra.[34] However, in practice, the measurements are contaminated with noise. Therefore, the tensor decomposition is not exact but a CPD model is fitted to the observed tensor using numerical optimization, minimizing the model error. In such cases, uniqueness of the decomposition can be confirmed with respect to the fitted tensor only. Moreover, the algorithm may get stuck in a local minimum. In order to verify the reliability of the solution, the following sanity checks can be done:

Checking whether the estimated factors and rank comply with the uniqueness conditions cited in section *BSS Multiway Data*. Note that in the noisy case, these conditions are necessary but not sufficient anymore, as there is no way to verify that the fitted tensor is the true noiseless version of the observed tensor.

- Running the algorithm, several times, the consistency of the estimated factors can be verified. This can be done either visually, or, in case of large-scale problems with many components, in

a semi-automated way using clustering, in a similar fashion as done with ICASSO for ICA[35]

- Using different initialization strategies,[36] to make sure that the algorithm can converge to the global minimum and not get stuck in a local minimum.

Coming back to the previous example of Figure 2, we ran CPD ten times with different initialization strategies, once using generalized eigenvalue decomposition, 4 times randomly generated orthogonal factors and 5 times randomly generated factors. The resulting components were compared pairwise using Pearson's correlation coefficient. In all cases, a perfect correlation ($r = 1$) was found, suggesting that we have found a unique solution. Moreover, as none of the factors contain collinear columns (as verified by visual inspection as well as by a low Pearson's correlation value), each factor has k - rank = 2. Then, Eq. (3) holds as $R = 2$ and $2 + 2 + 2 \geq 2 \cdot 2 + 2$. The components emerging from this rank-2 CPD solution are visualized in the bottom left panel of Figure 2.

Once the reliability of the solution is confirmed, one needs to relate the various extracted components to physical sources. Sometimes background knowledge is sufficient to identify the sources, e.g., eye blink-related components are easily recognized due to their large contribution on the frontal EEG channel, such as the component on the right in of Figure 2(d). The component on the left is identified as a seizure based on background knowledge: epileptic seizures cause an oscillatory pattern in the EEG, such as the signal observed in the temporal signature of this component. In other cases, e.g., large number of components or lack of expert knowledge, supervised learning can be used to train a classifier on a set of known examples that can later select the sources of interest in new datasets.[37]

After matching the components to physical sources, the signatures can be used to characterize the sources or use the signatures as features for pattern recognition and clinical decision-making. This often implies some application-specific postprocessing step, some of which will be discussed in the following section.

Expert knowledge is crucial throughout the whole procedure, from the earliest step onwards. In our example, we choose the first 2 second of EEG segment, as this will allow us to characterize the seizure onset. The localization of the SOZ can be derived from the spatial signature of the component. As seen in Figure 2, the seizure is most prominent in the right frontotemporal area, which is in agreement with other clinical information of the patient. Nevertheless, the user may be interested in other sorts of information about the data, such as the evolution of the seizure pattern. It is then the user's responsibility to select an appropriate data segment and a tensor model which can characterize more complex patterns which vary in time. To illustrate such an exploratory analysis, we take the full 10-second long EEG segment and apply block term decomposition after wavelet transformation. In order to check whether the spectral content of the seizure evolves, one rank-1 component and one low-rank component is extracted using BTD-(L_r L_r,1), i.e., with $L_1 = 1$ but with $L_2 = 2$ in the time and frequency mode. The resulting components are visualized in Figure 5(a). One can see on the left that the seizure pattern, with very similar channel, frequency, and temporal signatures as in Figure 2, is represented in the rank-1 term. The other component on the right has a topography similar to eye blinks, however, its temporal signatures show both an oscillatory seizure-like pattern and eye blinks. It seems that the sources are not well separated, the chosen tensor structure is not appropriate for the data. This may indicate that the seizure and the eye blinks have a stable spectral content throughout the duration of the segment. Alternatively, to check whether the seizure pattern spreads through the brain, the channel and temporal signatures are defined as low rank with $L_2 = 2$. The results are shown in Figure 5(b). One can observe now on the left that the eye blink component is modeled in the rank-1 term. The low-rank seizure term, shown on the right, is characterized by an oscillatory pattern at 5 Hz. The spatial signatures indicate that, compared with the onset, the seizure pattern has propagated toward posterior temporal areas and in frontal areas as well.

TENSOR ANALYSIS OF EPILEPTIC EEG AND fMRI: SUCCESSFUL APPLICATIONS

Table 1 gives an overview about the studies in the literature, which have successfully applied tensor decompositions to analyze EEG and fMRI datasets and answer important clinical questions about epilepsy.

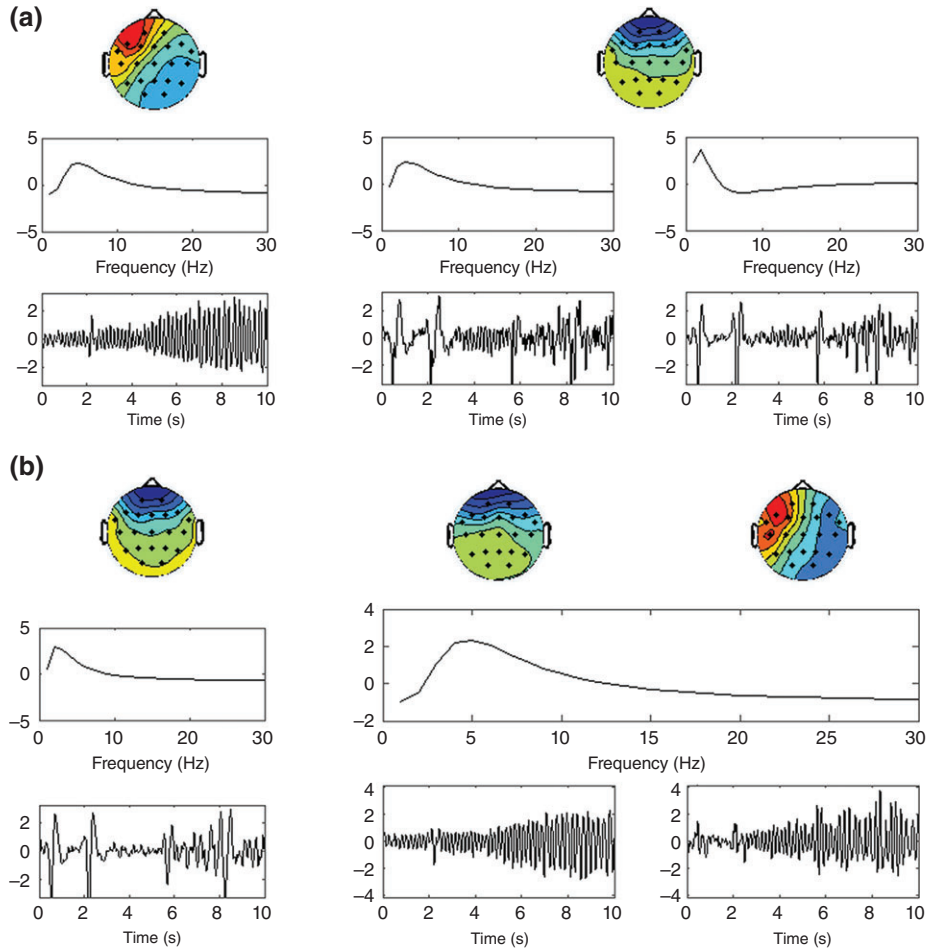

FIGURE 5 | (L,L,1)-Block term decomposition of the 10-second long EEG segment visualized in Figure 2. Low-rank components can model the temporal evolution of the seizure. In the examples shown, two components are extracted, a rank-1 component and a low-rank component with L = 2. (a) The frequency and the temporal modes are chosen to be low rank to explore whether the seizure changes in its spectral content. (b) The spatial and temporal modes are chosen to be low rank to explore whether the seizure spreads through the brain. EEG, electroencephalography.

EEG Analysis

As explained already in section *Mining EEG and fMRI in Epilepsy*, automated EEG analysis methods can assist visual inspection through extracting the pure epileptic activity patterns and rejecting artifacts, or reduce the workload of clinicians through automated seizure detection. Epileptic seizure patterns have been successfully retrieved using CPD of wavelet transformed multichannel EEG data.[27,28] Both applications rely on the assumption that the oscillatory seizure pattern remains stationary within a short observation window, maintaining the same frequency spectrum and localization. Therefore, its pattern is well represented with a rank-1 tensor, which is the outer product of an oscillatory temporal pattern, a frequency signature with a clear peak and with a channel signature. These signatures can be utilized in various ways. First, the component corresponding to epileptic activity has to be selected. This can be done by ordering the components according to their variance and excluding eye blink sources.[28] Then, the channel distribution can be postprocessed in order to localize the SOZ, by selecting those channels where the seizure pattern is dominant, i.e., present with amplitude higher than a predefined relative threshold.[28] This technique will reveal the SOZ in channel space. However, more precise spatial information can be obtained by utilizing source localization techniques on the channel signature,[45] which will pinpoint the SOZ in the so-called source space, defined as a 3D grid in the entire volume of the brain. Moreover, in a patient-

TABLE 1 | An Overview about the Studies in the Literature

Study	Application	Modality	Tensorization	Tensor Model	Postprocessing
[27]	Seizure onset zone localization	EEG	Wavelet transform	CPD	Visual analysis
[28]	Seizure onset zone localization	EEG	Wavelet transform	CPD	Component ordering and selection of dominant channels
[15]	Seizure onset localization	EEG	Hankel matrix representation	BTD	Visual assessment
[38]	Seizure detection	EEG	Wavelet transform	CPD	CPD of new segments using fixed spectral and spatial signatures, classification based on temporal signature
[39]	Seizure detection	EEG	Windowed spectrogram	Tucker	Classifier training on selected subsets of factors
[40]	Seizure detection	EEG	Time and frequency features	N-PLS	Classification using the component matrices from N-PLS model
[41]	Lateralization of the seizure onset	EEG	Graph features	Tucker	Analysis of residuals and hoteling *T*-squared values
[42]	Seizure prediction (modeling preictal period)	EEG	Relative power in sub-bands	CPD	Component selection based on correlation with target, visual analysis of signatures
[43]	Functional connectivity analysis	fMRI	Natural (voxels × time × patients)	CPD with independence constraint (T-PICA)	Component selection using regression to task time course; statistical analysis for group comparisons
[44]	Interictal network analysis	EEG–fMRI	Natural (channel × time × patient)	CMTF	Visual analysis

EEG, electroencephalography; fMRI, functional magnetic resonance imaging; CPD, canonical polyadic decomposition; BTD, block term decomposition; N-PLS, multiway partial least squares; CMTF, coupled matrix-tensor factorization; T-PICA, Tensor Probabilistic Independent Component Analysis.

specific setting, where the first seizure pattern serves as training data, the channel, time, and frequency signatures extracted by CPD can also be used as features to train a classifier and detect subsequent seizures.[38] Alternatively, a tensor can be built by extracting various discriminative time and frequency domain features, such as Hjorth parameter of spectral entropy from the multichannel EEG segments. Then, using labels from the training data, N-PLS-based multilinear regression is used to model the epilepsy feature tensor. Again, the extracted component can be used to predict the labels of new EEG segments from the same patient.[40] A recent study[39] has developed a framework based on Tucker decomposition, which allows to train classifiers sensitive to certain types of EEG patterns, by selecting subsets of the core tensor corresponding to relevant factor signatures. This is a step forward to patient independent seizure detection, as it enables the user to target specific types of epileptic patterns without collecting patient-specific data.

fMRI Analysis

Tensor-based solutions for fMRI data are scarce in the literature. Although fMRI images are inherently 3D, the spatial patterns of interest are usually not low rank in this space. Moreover, as the cortical surface is highly folded, neighboring voxels in the fMRI do not necessarily represent adjacent neuronal populations. Therefore, fMRI images are usually vectorized, and the consecutively recorded images are stored in a *voxels* × *time* matrix.

The ICA is a popular class of matrix-based BSS techniques, which is often used to analyze fMRI time series. It can delineate epileptic networks[37] and so-called resting state networks (RSNs) as well, which comprise various spontaneously coactivating brain regions.[46] Analysis of RSNs and the degree of

functional connectivity among the nodes of these networks is a very promising research area in epilepsy. The disruption of RSN functional connectivity in epilepsy patients gives us deeper insight in the disease mechanisms and the resulting clinical manifestations, such as decreased connectivity in the language network during rest in patients with language impairment.[47]

Functional connectivity studies compare the connectivity of a homogeneous group of patients against a group of individuals in order to retrieve robust and reproducible network connectivity patterns. Data from individual subjects can be organized in a *voxels* × *time* × *subject* tensor. The time course of network activity in resting state differs in each individual. However, in task-based fMRI, where each participant executes the same task protocol, the networks engaged by the task will have similar activation time course. Therefore, these sources will have a rank-1 structure and can be decomposed using CPD. Considering the success of the source independence constraint widely applied in fMRI research, Beckmann and Smith[48] have proposed tensor probabilistic ICA, which incorporates this constraint into the CPD model. Using this approach, previously unknown functional reorganization was discovered in a group of temporal lobe epilepsy cases.[43]

EEG–fMRI Analysis

Simultaneous EEG–fMRI has gained increasing importance in the past years, despite technical difficulties which arise due to the simultaneous measurements.[2] The motivation behind integrating these two modalities is their complementary nature. They not only record different aspects of neural activity, they can complement each other's temporal and spatial resolution. In the context of epilepsy, this tool is useful to delineate the irritative zone and some centers have already implemented this technique in clinical practice within presurgical evaluation.

Several ways exist to integrate information from EEG and fMRI data. Sequential integration means that the information from one modality is used to inform or constrain the analysis of the other, such as within the general linear model, in which the interictal spikes detected on EEG are used to obtain a regressor for the fMRI analysis.[49] The specificity and sensitivity, hence the successful clinical use of this technique, largely depends on correctly identifying interictal epileptic discharges on the EEG,[3] the use of an appropriate hemodynamic model and appropriate thresholding of the statistical maps.[50] General Linear Model (GLM) based maps often show widespread activation patterns, including voxels remote to the epileptogenic areas. This may be due to the fact that the EEG signals, used as a reference, represent a mixture of neural processes[51] or it may represent an underlying interictal network.[52]

Model-free, data-driven approaches can relax or circumvent some of the above difficulties. During parallel integration, each modality is first processed separately using ICA. Then, in a second phase, the sources are matched across the modalities.[51] The advantage of this approach is that the source signatures will not be affected by a possibly inaccurate model specification, e.g., inaccurate EEG information or hemodynamic model. Indeed, this technique helped the interpretation of widespread GLM-based epileptic activation maps to pinpoint the EZ.[44]

The drawback of parallel integration is that it does not allow a flow of information between the modalities, while this may enhance the discovery of interesting patterns, which are present in both datasets. Symmetric EEG–fMRI fusion processes the modalities simultaneously, allowing a flow of information in both directions. As such, jointICA of EEG–fMRI can give a detailed spatiotemporal characterization of the neural processing, taking the best of both worlds.[8,18] An extension of this technique allows incorporating multichannel EEG information by temporal or spatial concatenation.[53] In either case, however, the spatial or temporal interdependencies of the multichannel signals are lost. In order to exploit the inherent higher dimensional structure of the EEG, a tensor representation and joint matrix-tensor decomposition is preferred. Indeed, the superiority of this approach over jointICA and multichannel jointICA has been shown in a recent study[44] revealing an interesting association between different features within an interictal epileptic discharge and different fMRI activation clusters

CONCLUSION

Tensor decompositions are a very powerful set of tools for BSS of functional neural datasets. Their power relies on two principles. First, tensor representations allow to exploit the inherent higher dimensional structure of EEG and fMRI data. Second, tensor decompositions offer a unique solution under mild conditions, which allows unambiguous interpretation of the signatures. Therefore, we presented a general framework for tensor-based EEG–fMRI

signal processing, explaining the most important considerations to make during each step of the processing pipeline and discussed successful applications in epilepsy.

ACKNOWLEDGMENTS

The authors would like to thank the anonymous reviewers for their valuable suggestions. The research leading to these results has received funding from the European Research Council under the European Union's Seventh Framework Programme (FP7/2007-2013)/ERC Advanced Grant: BIOTENSORS (n° 339804). This paper reflects only the authors' views and the Union is not liable for any use that may be made of the contained information. We also acknowledge financial support from the following organizations: iMinds Medical Information Technologies: Dotatie-Strategisch basis onderzoek (SBO- 2016); Belgian Federal Science Policy Office: IUAP #P7/19/ (DYSCO, 'Dynamical systems, control and optimization', 2012-2017)

FURTHER READING

Cong F, Lin QH, Kuang LD, Gong XF, Astikainen P, Ristaniemi T. Tensor decomposition of EEG signals: a brief review. *J Neurosci Methods* 2015, 248:59–69.

Lahat D, Adali T, Jutten C. Multimodal data fusion: an overview of methods, challenges, and prospects. *Proc IEEE* 2015, 103.9: 1449–1477. http://ieeexplore.ieee.org/stamp/stamp.jsp?arnumber=7214350.

Mørup M. Applications of tensor (multiway array) factorizations and decompositions in data mining. *WIREs: Data Mining Knowl Discov* 2011, 1:24–40.

Stern J, Engel J. *An Atlas of EEG Patterns*. Philadelphia, PA: Lippicott; 2004.

REFERENCES

1. Strobbe G, Carrette E, López J, Van Roost D, Meurs A, Vonck K, Boon P, Vandenberghe S, van Mierlo P. Electrical source imaging of interictal spikes using multiple sparse volumetric priors for presurgical epileptogenic focus localization. *Neuroimage Clin* 2016, 11:252–263.
2. Vanderperren K, De Vos M, Ramautar J, Novitskiy N, Mennes M, Assecondi S, Vanrumste B, Stiers P, Van den Bergh B, Wagemans J, et al. Removal of BCG artifacts from EEG recordings inside the MR scanner: a comparison of methodological and validation-related aspects. *Neuroimage* 2010, 50:920–934.
3. Tousseyn S, Dupont P, Robben D, Goffin K, Sunaert S, Van Paesschen W. A reliable and time-saving semiautomatic spike-template-based analysis of interictal EEG–fMRI. *Epilepsia* 2014, 55:2048–2058.
4. Liston A, De Munck J, Hamandi K, Laufs H, Ossenblok P, Duncan J, Lemieux L. Analysis of EEG–fMRI data in focal epilepsy based on automated spike classification and signal space projection. *Neuroimage* 2006, 31:1015–1024.
5. Karahan E, Rojas-Lopez P, Bringas-Vega M, Valdes-Hernandez P, Valdes-Sosa P. Tensor analysis and fusion of multimodal brain images. *Proc IEEE* 2015, 103:1531–1559.
6. Lu Y, Bagshaw A, Grova C, Kobayashi E, Dubeau F, Gotman J. Using voxel-specific hemodynamic response function in EEG–fMRI data analysis. *Neuroimage* 2006, 32:238–247
7. van Mierlo P, Carrette E, Hallez H, Vonck K, Van Roost D, Boon P, Staelens S. Accurate epileptogenic focus localization through time-variant functional connectivity analysis of intracranial electroencephalographic signals. *Neuroimage* 2011, 56:1122–1133.
8. Centeno M, Carmichael DW. Network connectivity in epilepsy: resting state-fMRI and EEG–fMRI contributions. *Front Neurol* 2014, 5:9.
9. Richardson M. Current themes in neuroimaging of epilepsy: brain networks, dynamic phenomena, and clinical relevance. *Clin Neurophysiol* 2010, 121:1153–1175.
10. De Lathauwer L. A short introduction to tensor-based methods for factor analysis and blind source separation. In: *7th International Symposium on Image and Signal Processing and Analysis*, Dubrovnik, Croatia, 2011 December.
11. Kruskal J. Three-way arrays: rank and uniqueness of trilinear decompositions, with applications to arithmetic complexity and statistics. *Linear Algebra Appl* 1977, 18:95–183.

12. Sidiropoulos N, Bro R. On the uniqueness of multilinear decomposition of N-way arrays. *J Chemometr* 2000, 14:229–239.

13. Domanov I, De Lathauwer L. On the uniqueness of the canonical polyadic decomposition of third-order tensors—part I: basic results and uniqueness of one factor matrix. *SIAM J Matrix Anal Appl* 2013, 34:855–875.

14. Domanov I, De Lathauwer L. On the uniqueness of the canonical polyadic decomposition of third-order tensors—part II: overall uniqueness. *SIAM Matrix Anal Appl* 2013, 34:876–903.

15. Hunyadi B, Camps D, Sorber L, Van Paesschen W, De Vos M, Van Huffel S, De Lathauwer L. Block term decomposition for modelling epileptic seizures. *EURASIP J Adv Signal Process* 2014, 139:1–19.

16. De Lathauwer L. Decompositions of a higher-order tensor in block terms—part II: definitions and uniqueness. *SIAM J Matrix Anal Appl* 2008, 30:1033–1066.

17. De Lathauwer L. Blind separation of exponential polynomials and the decomposition of a tensor in rank-(Lr, Lr, 1) terms. *SIAM J Matrix Anal Appl* 2011, 32:1451–1474.

18. Calhoun V, Adali T, Pearlson G, Kiehl K. Neuronal chronometr of target detection: fusion of hemodynamics and event-related potential data. *Neuroimage* 2006, 30:544–553.

19. Mijovic B, Vanderperren K, Novitskiy N, Vanrumste B, Stiers P, Van den Bergh B, Lagae L, Sunaert S, Wagemans J, Van Huffel S. The why and how of jointICA: results from a visual detection task. *Neuroimage* 2012, 60:1171–1185.

20. Sui J, Pearlson G, Adali T, Kiehl K, Caprihan A, Liu J, Yamamoto J, Calhoun V. Discriminating schizophrenia and bipolar disorder by fusing fMRI and DTI in a multimodal CCA+ joint ICA model. *Neuroimage* 2011, 57:839–855.

21. Sorensen M, De Lathauwer L. Coupled canonical polyadic decompositions and (coupled) decompositions in multilinear rank-(Lr,n, Lr,n, 1) terms—part I: uniqueness. *SIAM J Matrix Anal Appl* 2015, 36:496–522.

22. Acar E, Papalexakis E, Gürdeniz G, Rasmussen M, Lawaetz A, Nilsson M, Bro R. Structure revealing data fusion. *BMC Bioinformatics* 2014, 15:239.

23. Rivet B, Duda M, Guérin-Dugué A, Jutten C, Comon P. Multimodal approach to estimate the ocular movements during EEG recordings: a coupled tensor factorization method. In: *37th Annual International Conference of the IEEE Engineering in Medicine and Biology Society (EMBC)*, Milan, Italy, August 2015.

24. Martinez-Montes E, Valdes-Sosa P, Miwakeichi F, Goldman R, Cohen M. Concurrent EEG/fMRI analysis by multiway partial least squares. *Neuroimage* 2004, 26:973.

25. Vervliet N, Debals O, Sorber L, Van Barel M De Lathauwer L. Tensorlab 3.0. [Online]. Available at: http://www.tensorlab.net/. (Accessed 14 October 2016).

26. Andersson C, Bro R. The N-way toolbox for MATLAB. *Chemomet Intell Lab Syst* 2000, 52:1–4.

27. Acar E, Aykut-Bingol C, Bingol H, Bro R, Yener B. Multiway analysis of epilepsy tensors. *Bioinformatics* 2007, 23:i10–i18.

28. De Vos M, Vergult A, De Lathauwer L, De Clercq W, Van Huffel S, Dupont P, Palmini A, Van Paesschen W. Canonical decomposition of ictal scalp EEG reliably detects the seizure onset zone. *Neuroimage* 2007, 37:844–854.

29. Debals O, De Lathauwer L. Stochastic and deterministic tensorization for blind signal separation. In: *Latent Variable Analysis and Signal Separation*. Lecture Notes in Computer Science, vol. 9237, 2015, 3–13.

30. Timmerman M, Kiers H. Three-mode principal components analysis: choosing the numbers of components and sensitivity to local optima. *Br J Math Stat Psychol* 2000, 53:1–16.

31. Bro R, Kiers H. A new efficient method for determining the number of components in PARAFACmodels. *J Chemometr* 2003, 17:274–286.

32. Miwakeichi F, Martınez-Montes E, Valdés-Sosa P, Nishiyama N, Mizuhara H, Yamaguchi Y. Decomposing EEG data into space–time–frequency components using parallel factor analysis. *Neuroimage* 2004, 22:1035–1045.

33. Latchoumane C, Vialatte F, Solé-Casals J, Maurice M, Wimalaratna S, Hudson N, Jeong J, Cichocki A. Multiway array decomposition analysis of EEGs in Alzheimer's disease. *J Neurosci Methods* 2012, 207:41–50.

34. Cichocki A, Mandic D, De Lathauwer L, Zhou G, Zhao Q, Caiafa C, Phan H. Tensor decompositions for signal processing applications: from two-way to multiway component analysis. *Signal Process Mag* 2015, 32:145–163.

35. Himberg J, Hyvarinen A. ICASSO: software for investigating the reliability of ICA estimates by clustering and visualization. In: *IEEE 13th Workshop on Neural Networks for Signal Processing*, Tolouse, France, September 2013.

36. Sorber L, Van Barel M, De Lathauwer L. Optimization-based algorithms for tensor decompositions: canonical polyadic decomposition, decomposition in rank-(Lr , Lr , 1) terms and a new generalization. *SIAM J Optim* 2013, 23:695–720.

37. Hunyadi B, Tousseyn S, Dupont P, Van Huffel S, De Vos M, Van Paesschen W. A prospective fMRI-based technique for localising the epileptogenic zone in presurgical evaluation of epilepsy. *Neuroimage* 2015, 113:329–339.

38. Ontivero-Ortega M, Garcia-Puente Y, Martínez-Montes E. Comparison of classifiers to detect epileptic

seizures via PARAFAC decomposition. In: *VI Latin American Congress on Biomedical Engineering*, Paraná, Argentina, 2014.

39. Spyrou L, Kouchaki S, Sanei S. Multiview classification of brain data through tensor factorisation. In: *IEEE 25th International Workshop on Machine Learning for Signal Processing (MLSP)*, Boston, USA, 2015.
40. Acar E, Aykut-Bingol C, Bingol H, Bro R, Yener B. Seizure recognition on epilepsy feature tensor. In: *Conference Proceedings of the IEEE Engineering in Medicine and Biology Conference*, Lyon, France, August 2007.
41. Dhulekar N, Oztan B, Yener B, Bingol HO, Irim G, Aktekin B, Aykut-Bingöl C. Graph-theoretic analysis of epileptic seizures on scalp EEG recordings. In: *Proceedings of the 5th ACM Conference on Bioinformatics, Computational Biology, and Health Informatics*, Newport, September 2014.
42. Direito B, Teixeira C, Ribeiro B, Castelo-Branco M, Dourado A. Space Time Frequency (STF) code tensor for the characterization of the epileptic preictal stage. In: *34th Annual International Conference of the IEEE EMBS*, San Diego, CA, USA, August 2012, 621–624.
43. Voets NL, Adcock JE, Stacey R, Hart Y, Carpenter K, Matthews PM, Beckmann C. Functional and structural changes in the memory network associated with left temporal lobe epilepsy. *Hum Brain Mapp* 2009, 30:4070–4081.
44. Hunyadi B, Van Paesschen W, De Vos M, Van Huffel M. Fusion of electroencephalography and functional magnetic resonance imaging to explore epileptic network activity. In: *24th European Signal Processing Conference (EUSIPCO)*, Budapest, Hungary, August 2016.
45. Becker H, Albera L, Comon P, Haardt M, Birot G, Wendling F, Gavaret M, Bénar CG, Merlet I. EEG extended source localization: tensor-based vs. conventional methods. *Neuroimage* 2014, 96:143–157.
46. De Luca M, Beckmann C, De Stefano N, Matthews P, Smith S. fMRI resting state networks define distinct modes of long-distance interactions in the human brain. *Neuroimage* 2006, 29:1359–1367.
47. Waites AB, Briellmann RS, Saling MM, Abbott DF, Jackson GD. Functional connectivity networks are disrupted in left temporal lobe epilepsy. *Ann Neurol* 2006, 59:1531–8249.
48. Beckmann C, Smith S. Tensorial extensions of independent component analysis for multisubject FMRI analysis. *Neuroimage* 2005, 25:294–311.
49. Gotman J. Epileptic networks studied with EEG-fMRI. *Epilepsia* 2008, 49:42–51.
50. Tousseyn S, Dupont P, Goffin K, Sunaert S, Van Paesschen W. Sensitivity and specificity of interictal EEG–fMRI for detecting the ictal onset zone at different statistical thresholds. *Front Neurol* 2014, 5:131.
51. Eichele T, Calhoun VD, Moosmann M, Specht K, Jongsma ML, Quiroga RQ, Hugdahl K. Unmixing concurrent EEG–fMRI with parallel independent component analysis. *Int J Psychophysiol* 2008, 67:222–234.
52. Tousseyn S, Dupont P, Goffin K, Sunaert S, Van Paesschen W. Correspondence between large-scale ictal and interictal epileptic networks revealed by single photon emission computed tomography (SPECT) and electroencephalography (EEG)–functional magnetic resonance imaging (fMRI). *Epilepsia* 2015, 56:382–392.
53. Swinnen W, Hunyadi B, Acar E, Van Huffel S, De Vos M. Incorporating higher dimensionality in joint decomposition of EEG and fMRI. In: *22nd European Signal Processing Conference (EUSIPCO)*, Lisbon, Portugal, September 2014.